SUPPLEMENTARY INFORMATION

Title: Advanced physiological maturation of human iPSC-derived cardiomyocytes using an algorithm-directed optimization of defined media components

Authors: Neal I. Callaghan *[1,2]†, Lauren J. Durland [1,3], Wenliang Chen [4#], Uros Kuzmanov [1,5], Maria Zena Miranda [1], Yu Ding [1,2], Zahra Mirzaei [1,2], Ronald G. Ireland [1,2], Cristine Reitz [1,5], Renée A. Gorman [4], Erika Yan Wang [2], Karl Wagner [2], Michelle M. Kim [2], Julie Audet [2,6], J. Paul Santerre [1,2,7], Anthony O. Gramolini [1,5], Filio Billia [8,9,10,11], Milica Radisic [2,6], Seema Mital [8,9,12,13], James Ellis [14,15], Peter H. Backx [4], and Craig A. Simmons *[1,2,16]

Affiliations:

[1] Translational Biology and Engineering Program, Ted Rogers Centre for Heart Research, Toronto, Ontario M5G 1M1, Canada

[2] Institute of Biomedical Engineering, Faculty of Applied Science and Engineering, University of Toronto, Toronto, Ontario M5S 3G9, Canada

[3] Department of Molecular Genetics, Temerty Faculty of Medicine, University of Toronto, Toronto, Ontario M5S 1A8, Canada

[4] Department of Biology, York University, Toronto, Ontario, Canada

[5] Department of Physiology, Faculty of Medicine, University of Toronto, Toronto, Ontario M5S 1A8, Canada

[6] Department of Chemical Engineering, Faculty of Applied Science and Engineering, University of Toronto, Toronto, Ontario M5S 3E5, Canada

[7] Faculty of Dentistry, University of Toronto, Toronto, Ontario M5G 1G6, Canada

[8] Ted Rogers Centre for Heart Research, Toronto, Ontario M5G 1M1, Canada

[9] Temerty Faculty of Medicine, University of Toronto, Toronto, Ontario M5S 1A8, Canada

[10] Division of Cardiology, Peter Munk Cardiac Centre, University Health Network, Toronto, Ontario M5G 2C4 Canada

[11] Toronto General Hospital Research Institute, University Health Network, Ontario M5G 2C4 Canada

[12] Department of Paediatrics, University of Toronto, Toronto, Ontario M5G 1X8, Canada

[13] Genetics and Genome Biology, The Hospital for Sick Children, Toronto, Ontario M5G 0A4, Canada

[14] Developmental and Stem Cell Biology, The Hospital for Sick Children, Toronto, Ontario M5G 0A4, Canada

[15] Department of Molecular Genetics, University of Toronto, Toronto, Ontario M5S 1A8, Canada.

[16] Department of Mechanical and Industrial Engineering, Faculty of Applied Science and Engineering, Toronto, Ontario M5S 3G8, Canada

† Current affiliation: Faculty of Medicine, Dalhousie University, Halifax, Nova Scotia B3H 4R2, Canada

Current affiliation: Translational Medicine Center, the Second Affiliated Hospital of Guangdong Medical University, Guangdong Medical University, Zhanjiang, Guangdong, China

*Corresponding authors: neal.callaghan@dal.ca; c.simmons@utoronto.ca

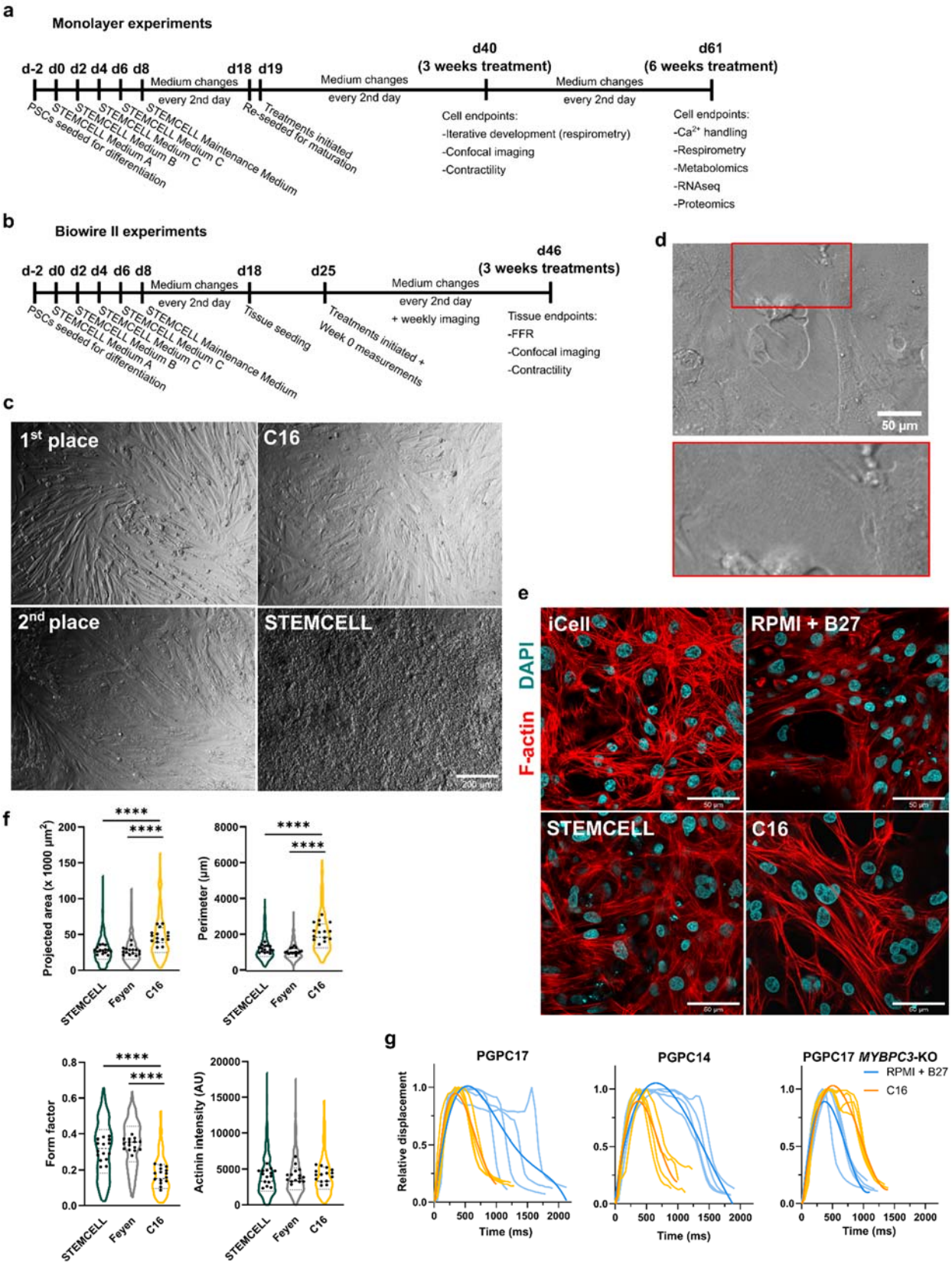
a
Monolayer experiments
d-2 d0 d2 d4 d6 d8
d18 d19
d40
(3 weeks treatment)
d61
(6 weeks treatment)
Medium changes every 2nd day
PSCs seeded for differentiation
STEMCELL Medium A
STEMCELL Medium B
STEMCELL Medium C
STEMCELL Maintenance Medium
Re-seeded for maturation
Treatments initiated
Cell endpoints:
-Iterative development (respirometry)
-Confocal imaging
-Contractility
Cell endpoints:
-Ca2+ handling
-Respirometry
-Metabolomics
-RNAseq
-Proteomics
b
Biowire II experiments
d-2 d0 d2 d4 d6 d8
d18
d25
d46
(3 weeks treatments)
Medium changes every 2nd day
+ weekly imaging
Tissue seeding
Week 0 measurements
Tissue endpoints:
-FFR
-Confocal imaging
-Contractility
c
1st place
C16
2nd place
STEMCELL
d
50 µm
e
iCell
RPMI + B27
STEMCELL
C16
DAPI
F-actin
f
Projected area (x 1000 µm2)
Perimeter (µm)
Form factor
Actinin intensity (AU)
STEMCELL
Feyen
C16
****
g
PGPC17
PGPC14
PGPC17 MYBPC3-KO
RPMI + B27
C16
Relative displacement
Time (ms)

Supplementary Figure 1. Experimental design, and morphology and performance of maturing hiPSC-CM monolayers. a) Timeline of hiPSC-CM differentiation, replating, monolayer treatment, and live analysis or harvesting for experiments described in the study. **b)** Timeline of hiPSC-CM differentiation, Biowire II seeding, treatment, and live analysis or harvesting for experiments described in the study. **c)** Relief contrast microscopy reveals spontaneous elongation and local alignment of hiPSC-CMs cultured 3 weeks in candidate maturation medium formulations (1st and 2nd place formulations by uncoupled:control ratio (UCR) metric in the iterative optimization process, and C16 medium) and STEMCELL Technologies Cardiomyocyte Maintenance Medium as a commercially-available high-performing control; scale bars represent 200 µm. **d)** hiPSC-CMs cultured 3 weeks in C16 medium have sarcomeric striations visible under brightfield microscopy; inset shows increased magnification to highlight striations. **e)** F-actin striation and bundling (red) visualized by phalloidin staining (DAPI in cyan) in cells cultured in C16 medium vs. iCell Cardiomyocytes Maintenance Medium, homemade RPMI + B27, or STEMCELL medium; scale bars represent 50 µm. **f)** Morphometric analyses of STEMCELL-, Feyen maturation media-, and C16-treated monolayer cultures, including projected area, perimeter, form factor, and integrated density of α-actinin signal under confocal microscopy. Violin plots represent technical replicate distribution; points represent biological replicates (n = 15 per treatment); due to differences in cell projected area, different numbers of cells were analyzed between treatments and samples. Actinin intensity $p = 0.91$; otherwise **** denotes $p < 0.0001$. Normality was tested using a D'Agostino and Pearson test, and conditions compared using a 1-way ANOVA with Tukey's post-hoc test. **g)** Normalized displacement curves of spontaneously-contracting C16- or RPMI + B27-treated hiPSC-CM monolayers (individual traces pale, n = 4 biologically independent replicates per treatment; quartic fits dark) derived from PGPC17, PGPC14, and PGPC17-*MYBPC3*-KO hiPSC lines. All analyses performed after 3 weeks of treatment with medium formulations. Micrographs demonstrative of at least 6 independent experiments each.

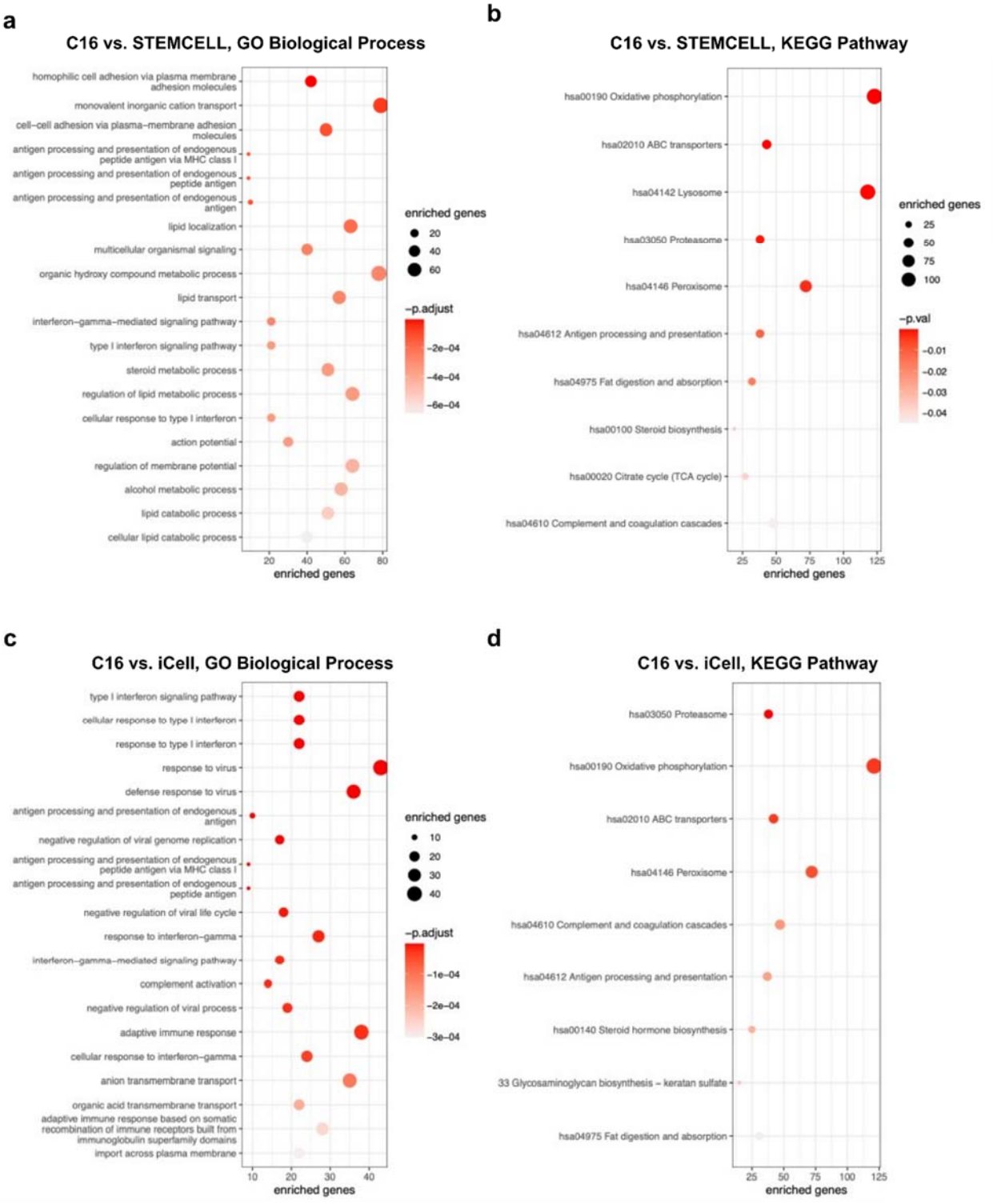

Supplementary Figure 2. Transcriptionally-enriched functional terms and pathways in C16-treated hiPSC-CMs. **a)** Top 20 enriched GO Biological Process terms among significantly upregulated genes in the indicated comparisons. Point size denotes the number of significantly upregulated genes in each enriched category. **b)** Top 20 enriched KEGG pathways in the indicated comparisons. Point size denotes the size of each gene set.

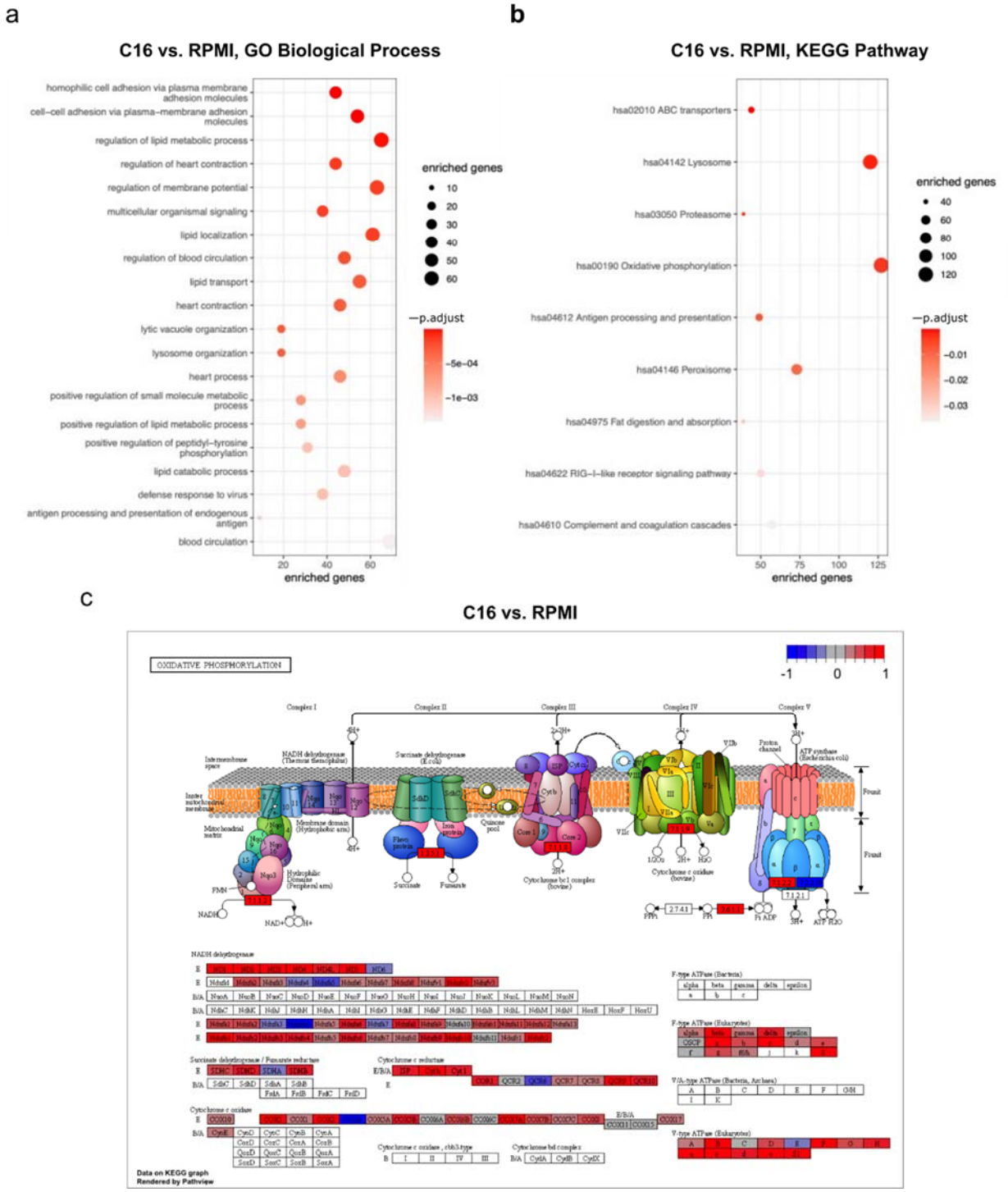

Supplementary Figure 3. Transcriptionally-enriched functional terms and pathways in hiPSC-CMs treated with C16 maturation medium. a) Top 20 enriched GO Biological Process terms among significantly upregulated genes in the indicated comparisons. Point size denotes the size of the enriched gene set corresponding to each term. **b)** Top 20 enriched KEGG pathways in the indicated comparisons. Point size denotes the size of the enriched gene set corresponding to each pathway. **c)** Schematic representation of the oxidative phosphorylation pathway (KEGG hsa000190) and corresponding gene expression data in C16 vs. treated hiPSC-CMs. Color denotes $\log_2$ fold change relative to control.

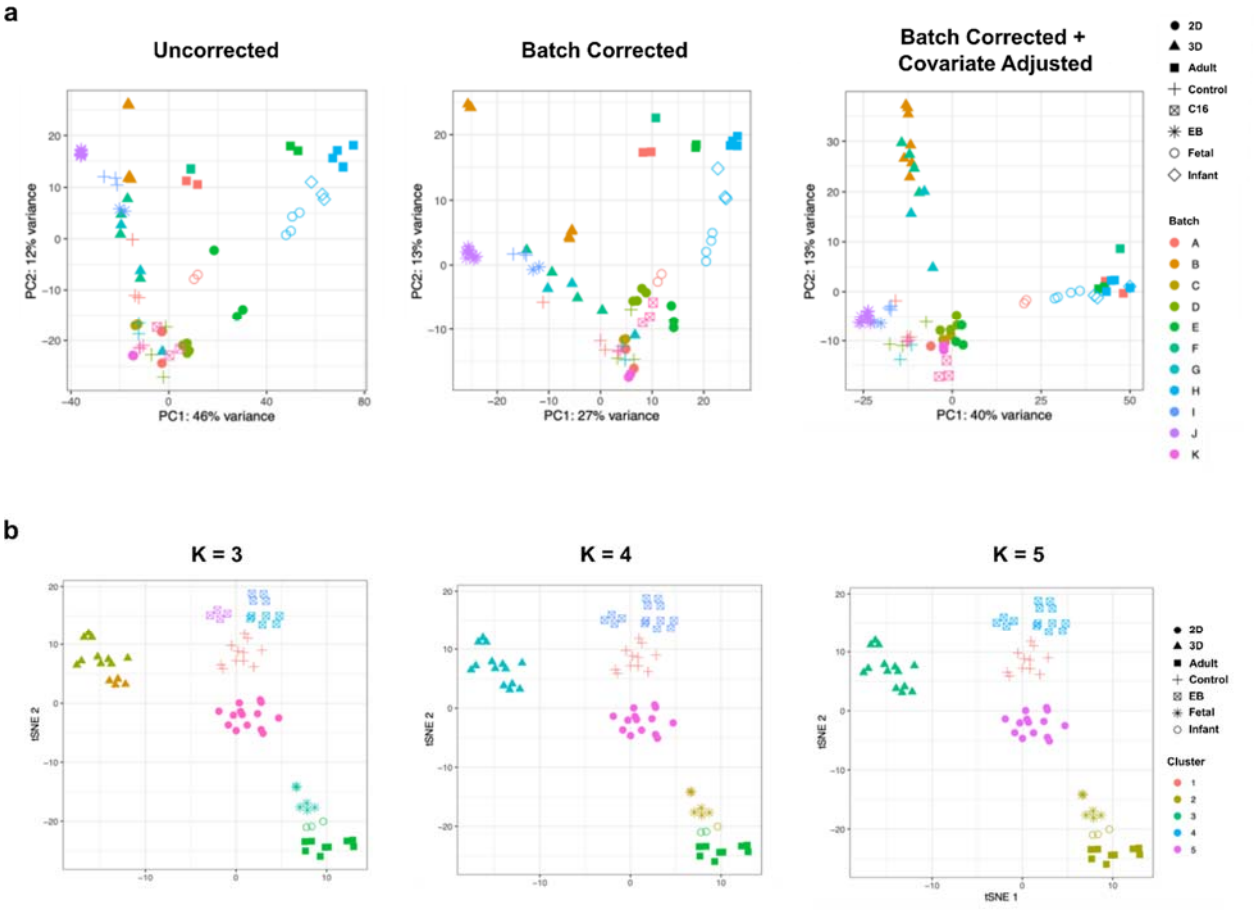

Supplementary Figure 4. Validation of RNA-seq meta-analysis workflow. a) Principal component analysis of meta-analysis samples without batch correction (left), with batch correction only (middle), or with batch correction and specification of 'type' as a covariate parameter (right). Color denotes batch, and shape denotes sample type. See **Supplementary Table 3** for assignment of samples to batches. **b)** tSNE plots displaying assignment of samples to clusters, using different k-values for construction of the k-nearest neighbour graph. Color denotes assigned cluster, and shape denotes sample type.

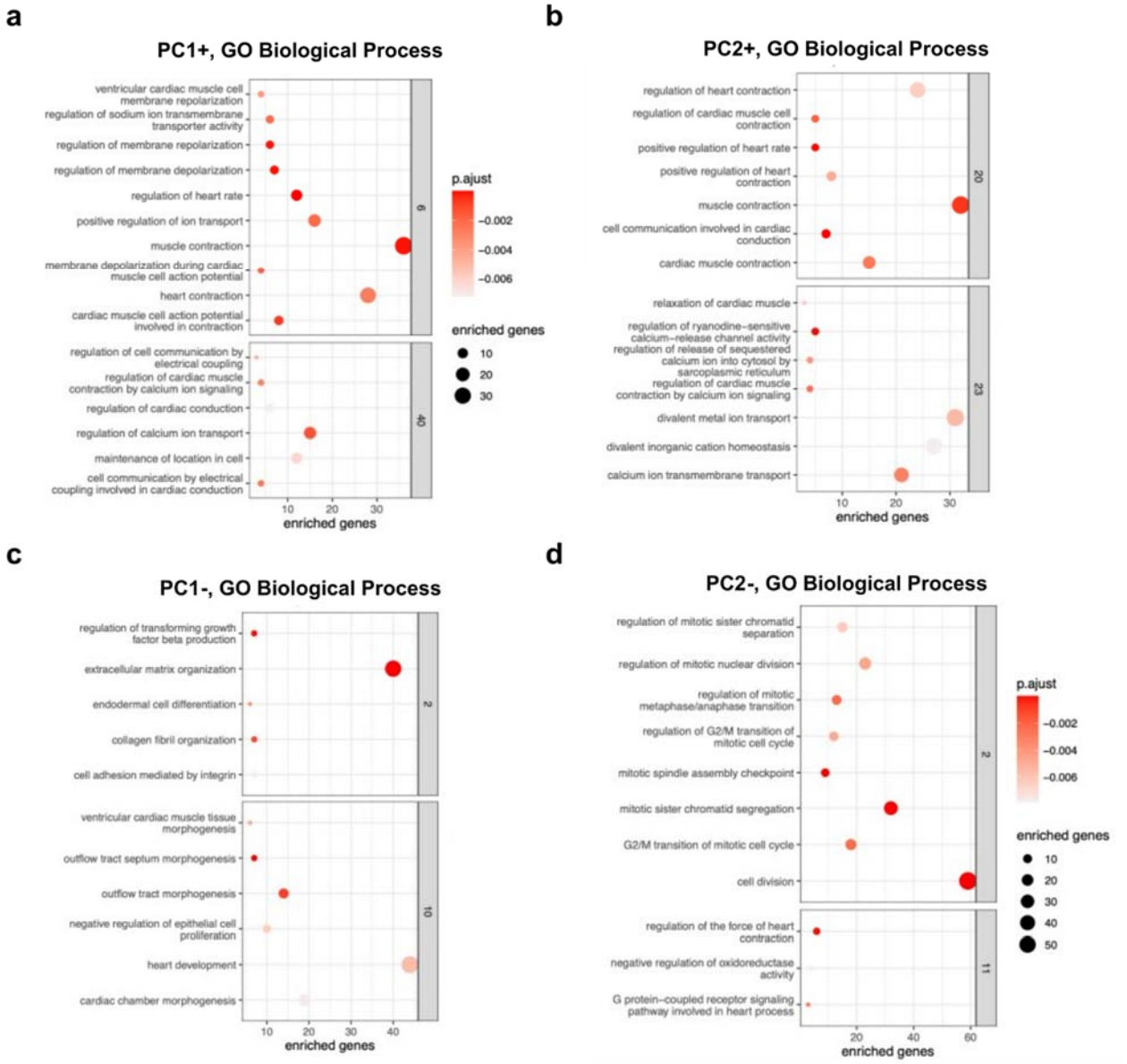

Supplementary Figure 5. Meta-analysis of hiPSC-CM maturation methods and *in vitro* myocardial development. Select clusters of enriched GO biological process terms corresponding to the indicated loadings within the principal component meta-analysis (**Figure 4l**) for PC1 **(a, c)** and PC2 **(b, d)**, positive **(a, b)**, and negative **(c, d)**. Point size denotes the size of the enriched gene set corresponding to each term. **Supplementary Table 3** includes detailed descriptions and references for each category.

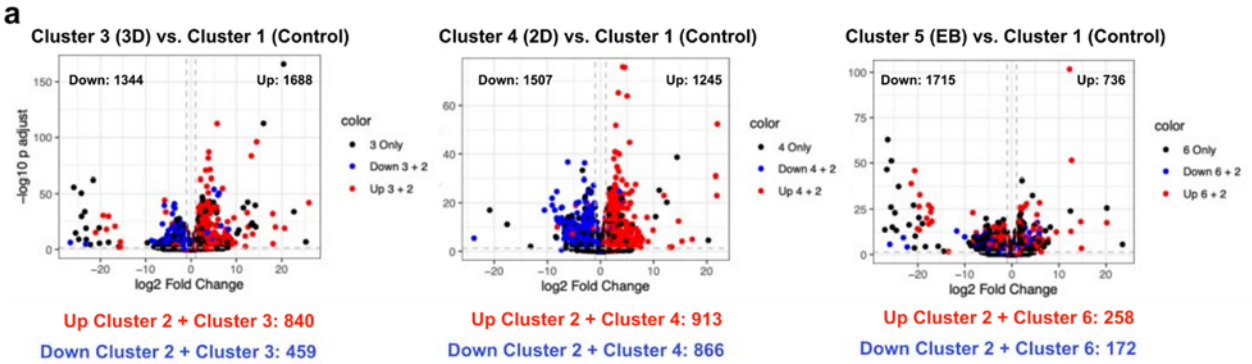

Up Cluster 2 + Cluster 3: 840

Down Cluster 2 + Cluster 3: 459

Up Cluster 2 + Cluster 4: 913

Down Cluster 2 + Cluster 4: 866

Up Cluster 2 + Cluster 6: 258

Down Cluster 2 + Cluster 6: 172

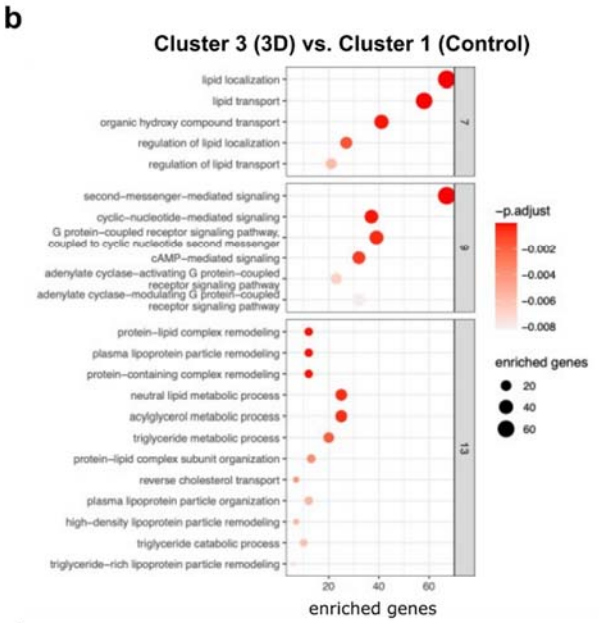

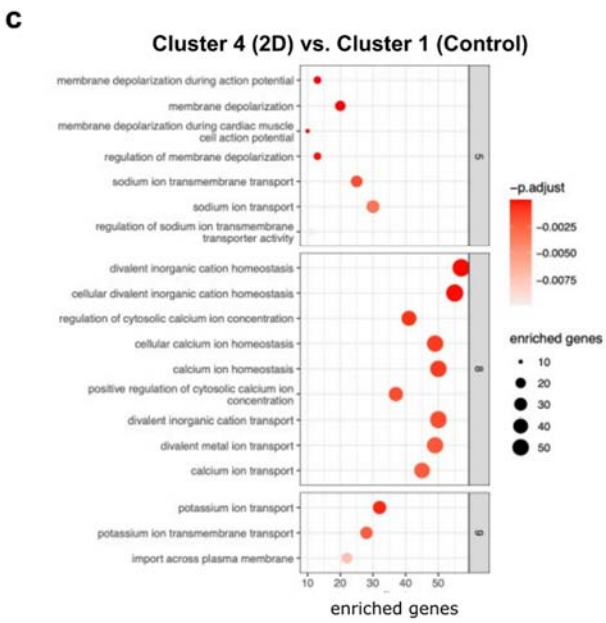

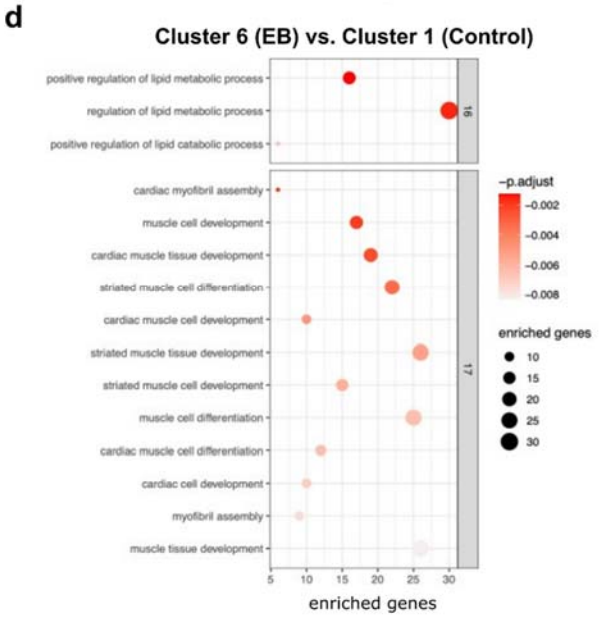

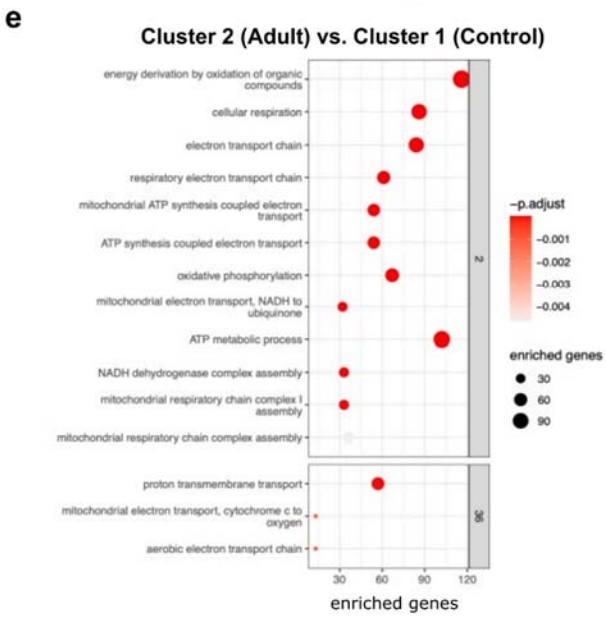

Supplementary Figure 6. Cluster comparisons from meta-analysis of RNAseq datasets from PSC-CM cultures and *in vivo* patient samples. a) Volcano plots displaying $\log_2$ fold changes and $\log_{10}$ adjusted p-values for each gene in the indicated comparisons. Grey dashed lines denote the threshold for statistical significance (log2 fold change > ± 1 and $p_{adj} < 0.05$). Red and blue points represent genes significantly upregulated and downregulated, respectively, in adult vs. control. The number of significantly upregulated genes in the indicated comparison, and both the indicated comparison and adult vs. control are listed below the corresponding graph. **b-e)** Select clusters of enriched GO biological process terms in the indicated comparisons. Point size denotes the size of the enriched gene set corresponding to each term.

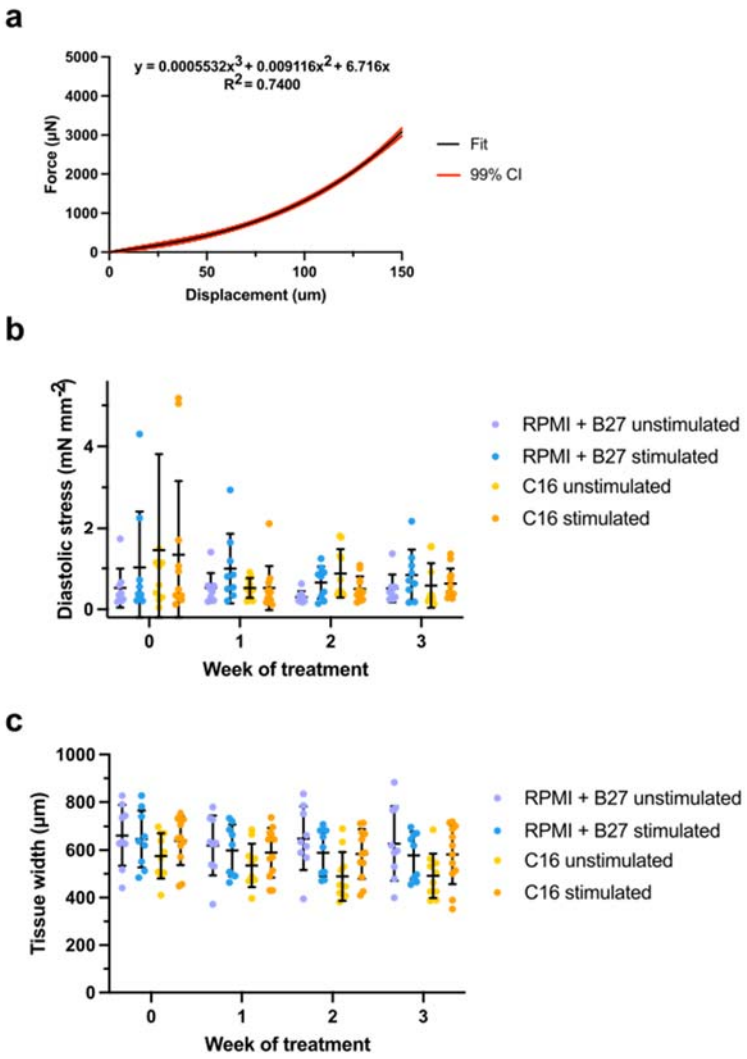

Supplementary Figure 7. Calibration and characterization of maturing engineered myocardial tissues (Biowire II cultures). a) Compliance curves (cubic fit; 99% CI denoted by red borders) demonstrate the force-displacement relationship used to calibrate tissue deflection of polymeric beams to absolute forces. **b)** Diastolic stress (passive tension normalized to cross-sectional area) of tissues did not differ between medium treatments or stimulation conditions. **c)** Time dependence of tissue width (top-down view) of tissues. No statistical significance by 2-way ANOVA in panels **b** or **c**; n = 9 for RPMI + B27 conditions and n= 10 and 12 for C16 unstimulated and stimulated conditions, respectively.

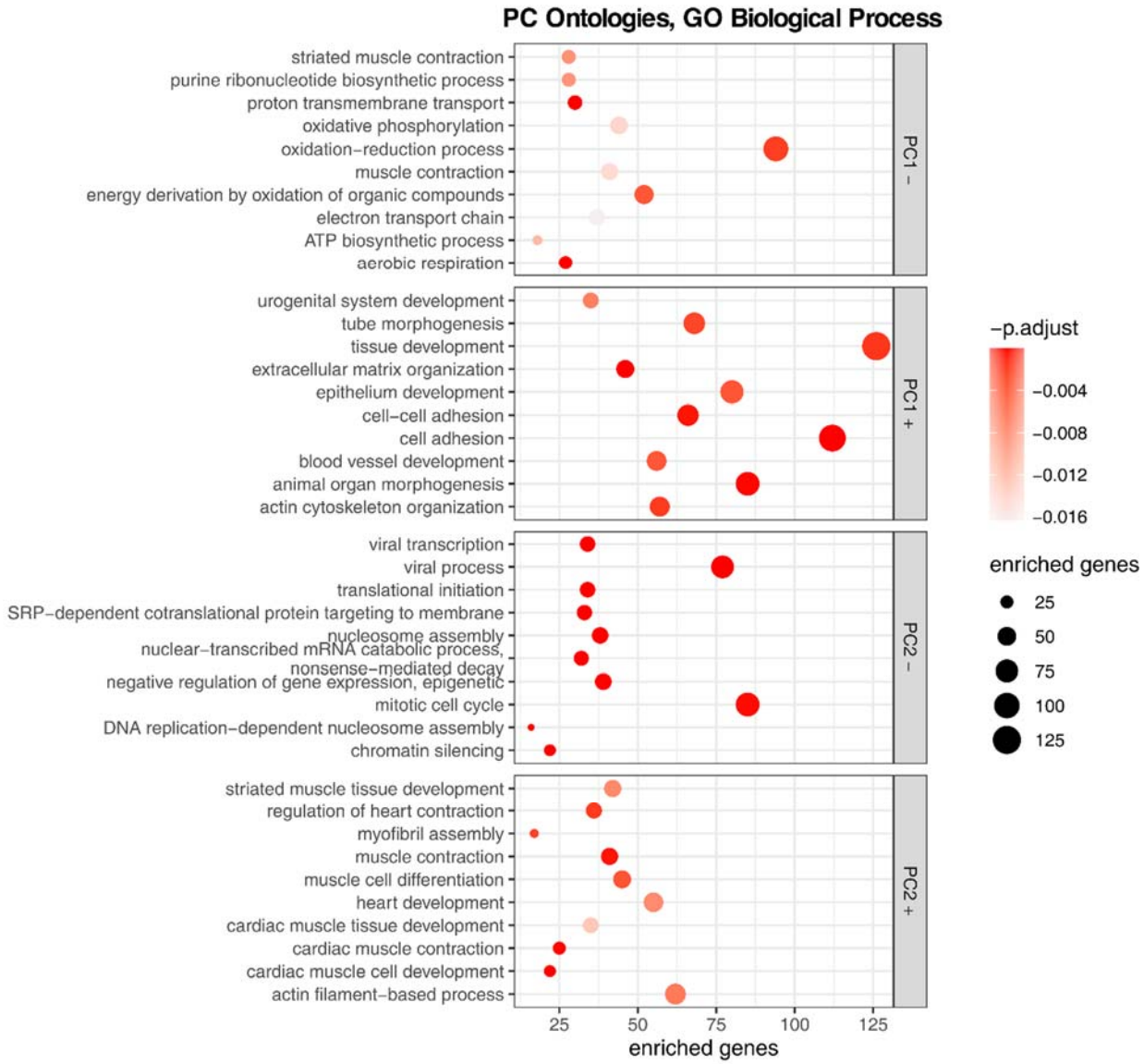

Supplementary Figure 8. Transcriptionally-enriched functional terms and pathways in C16-treated Biowire II cultures. Top 10 enriched GO Biological Process terms for each direction and principal component in bulk RNA sequencing of Biowire II cultures treated with C16 or RPMI + B27 media, with or without electrical stimulation (**Figure 6i**). Point size denotes the number of significantly upregulated genes in each enriched category.

Supplementary Table 1. Soluble factors used in iteration for inclusion in an M199-based HD-DE screen, with individual putative physiological effects, as well as references to previous use specifically in PSC-CM maturation, or general physiological effects. The bolded level is the effective concentration in C16 medium; order corresponds to labels of **Figure 1c**. Numerous studies have used RPMI + B27 supplement [1–8]; B27 additionally contains progesterone and pipecolic acid, which have no analogue in the compounds used in this study. Lactate and human growth hormone were not used in the final C16 formulation.

Label	Factor [concentration unit]	Present in B-27?	Concentration at each dose level					Utility	Previous use in CM maturation	General reference
			0	1	2	3	4			
A	2-deoxyglucose* [mmol L^{-1}]	No	0	2.0	3.16	**6.32**	20	Inhibits glycolysis, PPP/nucleotide metabolism, and hexosamine synthesis; Potential antiglycolytic synergies with insulin and metformin		9,10
B	Lactate [mmol L^{-1}]	No	**0**	1.0	1.58	3.16	10	Oxidative carbon source	11,12	11
C	Chemically-defined lipid** [X]	Yes, see note	0	**0.33**	0.52	1.04	3.3	Oxidative carbon source; Cholesterol maintains specialized membrane functionality and is a steroid precursor	Specific fatty acids [3,11–13]	
D	Galactose [mmol L^{-1}]	Yes	0	0.79	2.5	7.9	**25**	Carbon source; Inhibits lipotoxicity	12,13	14
E	Creatine-carnitine-taurine [X]	Yes	0	**0.1**	0.316	1	3.16	Creatine- local highly-available energy pool, regenerated between contractions; Carnitine- FA transit within cell; Taurine- redox-active, Ca homeostasis	Carnitine [15], CCT [8]	4,11,16–19
F	Insulin-Transferrin-Selenium (ITS)*** [X]	Yes, see note	0	**0.1**	0.316	1	3.16	Insulin- growth and differentiation signal; Transferrin- iron homeostasis; Selenium- Cofactor for redox processes		20
G	Albumin [mg mL^{-1}]	Yes	0	0.2	**0.316**	0.632	2	Hormone carrier; Lipid carrier	[Ubiquitous]	
H	β-mercaptoethanol† [µmol L^{-1}]	No, see note	0	10	15.81	31.6	**100**	Antioxidant	6	
I	Putrescine [mg mL^{-1}]	Yes	0	0.2	0.316	0.632	**2.0**	Polyamine effects on cell growth, proliferation, and hypertrophy; Maintenance of inward rectifying current; Protein stabilization; Excitation-contraction kinetic modulation		21–23
J	Ethanolamine [µmol L^{-1}]	Yes	0	**1**	3.16	10	31.6	Phospholipid precursor for electroactive membrane structure		24
K	Triiodothyronine [ng mL^{-1}]	Yes	0	**8**	12.65	25.3	80	Physiological cardiac hypertrophy and maturation	25–28	
L	Leukemia inhibitory factor [ng mL^{-1}]	No	0	0.6	0.949	1.897	**6**	Cardiomyocyte hypertrophy		29
M	Insulin-like growth factor [ng mL^{-1}]	No	0	10	15.81	**31.6**	100	Cell proliferation, growth, and survival	30	
N	Human growth hormone [ng mL^{-1}]	No	**0**	10	15.81	31.6	100	Cell hypertrophy; Protein synthesis; Oxidative metabolism; Attenuation of glycolytic pathways	31	
O	Hydrocortisone‡ [ng mL^{-1}]	No, see note	0	2.5	**7.91**	25	79.1	Glucocorticoid influence on cardiac maturation	27	
P	Neuregulin [ng mL^{-1}]	No	0	**0.1**	0.316	1	3.16	Cardiac maturation; Structural development and maintenance; Ca^{2+} homeostasis	30	32,33
Q	Metformin [µmol L^{-1}]	No	0	25	39.5	**79.1**	250	Increased catabolism through AMPK axis; Increased insulin sensitivity; Increased lipid catabolism; Inhibition of lipotoxicity; Ca^{2+} regulation		34

*2-deoxyglucose is omitted in co-culture applications, as it was found to be toxic at working concentrations to primary fibroblasts.

**B27 supplement contains oleic, linoleic, and linolenic acids but does not contain cholesterol, nor do most non-M199 basal media including DMEM and RPMI 1640. Maturation-specific citations in this table refer to experiments using any lipid as a carbon source.

***B27 supplement minus insulin supplements are often used in PSC-CM media. Transferrin is present in B-27. Selenium is present in both ITS and B-27 in the form of sodium selenite.

†B27 supplement contains catalase and superoxide dismutase for radical quenching rather than beta-mercaptoethanol, which may have toxic effects on certain cells.

‡B27 supplement contains corticosterone, which is a weakly active mineralcorticoid precursor to cortisol (hydrocortisone).

Supplementary Table 2. Clustering of high-performing candidate formulations and derivation of the C16 formulation. "Cluster" denotes placement in the PCA biplot (Fig. 1e); "X" denotes a formulation unassociated without a cluster. Letters above components denote the vector in the biplot.

Formulation	PCA cluster	Factor and dose level (defined in Supplementary Table 1)																
		A	B	C	D	E	F	G	H	I	J	K	L	M	N	O	P	Q
1	X	4	4	1	4	2	2	4	4	1	2	0	4	4	3	4	3	4
2	1	4	1	4	4	1	2	4	1	2	2	4	4	1	0	4	0	4
3	1	4	1	1	4	1	2	4	4	2	2	3	4	1	1	4	0	3
4	1	4	1	1	4	2	2	4	4	2	2	3	4	1	1	4	0	4
5	2	3	1	1	4	0	1	4	4	3	0	1	4	3	1	3	2	3
6	X	4	1	4	1	2	4	0	4	0	4	1	4	4	2	4	0	0
7	1	4	1	1	4	1	3	4	4	2	2	3	4	1	1	4	0	4
8	2	3	1	0	4	0	1	1	4	4	0	1	4	3	0	2	1	3
9	1	3	1	1	4	1	2	4	4	2	2	3	4	1	1	4	0	4
10	1	4	1	1	4	1	2	4	4	2	2	3	4	1	1	4	0	3
11	2	3	0	0	4	0	1	2	4	4	0	1	4	3	0	2	1	3
C16	2	3	0	1	4	1	1	2	4	4	1	1	4	3	0	2	1	3

Supplementary Table 3. Description of RNA-seq meta-analysis samples. "Adult", "Infant", and "Fetal" samples represent patient-derived myocardium or CM extracts thereof. "EB" samples represent PSC-CM differentiations and maturation in embryoid body format. "2D" samples represent matured PSC-CM monolayers, while "3D" samples represent engineered myocardial tissues. "Control" samples represent differentiated but unmatured PSC-CMs (*i.e.* harvested at the point of induction of maturation treatments).

Batch	Type	Description	Reference	GEO Accession
A	Control	Day 20 immature PSC-CM	[35]	GSE62913
	Fetal	Fetal cardiomyocyte, *in vivo*		
	Adult	Adult cardiomyocyte, *in vivo*		
	2D	PSC-CM in monolayer + let-7 overexpression		
B	3D	PSC-CM in ventricular Biowire, stimulated	[36]	GSE114976
	3D	PSC-CM in ventricular Biowire, non-stimulated		
C	2D	PSC-CM in monolayer + fatty acids	[15]	GSE124057
D	Control	Day 20 immature PSC-CM	[8]	GSE151279
	2D	PSC-CM in monolayer + complex defined maturation medium		
E	2D	PSC-CM in monolayer + 90 day culture period	[37]	GSE81585
	Adult	Adult cardiomyocyte, *in vivo*		
F	3D	PSC-CM in Heart-Dyno	[3]	GSE62913
	Control	Adult cardiomyocyte, *in vivo*		
G	3D	PSC-CM in organoid co-culture with fibroblasts/endothelial cells	[38]	GSE116464
	Control	Day 20 immature PSC-CM		
H	Fetal	Fetal cardiomyocyte, *in vivo*	[39]	PRJNA353755
	Adult	Adult cardiomyocyte, *in vivo*		
	Infant	Infant cardiomyocyte, *in vivo*		
I	EB	PSC-CM in EB + glucose deprivation	[40]	GSE84815
	Control	Day 20 immature PSC-CM		
J	EB	PSC-CM in EB + complex defined maturation medium	[41]	GSE125862

References

1. Correia, C. *et al.* 3D aggregate culture improves metabolic maturation of human pluripotent stem cell derived cardiomyocytes. *Biotechnol. Bioeng.* **115**, 630–644 (2018).
2. Ronaldson-Bouchard, K. *et al.* Advanced maturation of human cardiac tissue grown from pluripotent stem cells. *Nature* **556**, 239–243 (2018).
3. Mills, R. J. *et al.* Functional screening in human cardiac organoids reveals a metabolic mechanism for cardiomyocyte cell cycle arrest. *Proc. Natl. Acad. Sci. U. S. A.* **114**, E8372–E8381 (2017).
4. Bhute, V. J. *et al.* Metabolomics Identifies Metabolic Markers of Maturation in Human Pluripotent Stem Cell-Derived Cardiomyocytes. *Theranostics* **7**, 2078–2091 (2017).
5. Wong, A. O.-T. *et al.* Combinatorial Treatment of Human Cardiac Engineered Tissues With Biomimetic Cues Induces Functional Maturation as Revealed by Optical Mapping of Action Potentials and Calcium Transients. *Front. Physiol.* **11**, 1–11 (2020).
6. Sebastião, M. J. *et al.* Bioreactor-based 3D human myocardial ischemia/reperfusion in vitro model: a novel tool to unveil key paracrine factors upon acute myocardial infarction. *Transl. Res.* **215**, 57–74 (2020).
7. Stevens, K. R. *et al.* Physiological function and transplantation of scaffold-free and vascularized human cardiac muscle tissue. *Proc. Natl. Acad. Sci. U. S. A.* **106**, 16568–16573 (2009).
8. Feyen, D. A. M. *et al.* Metabolic Maturation Media Improve Physiological Function of Human iPSC-Derived Cardiomyocytes. *Cell Rep.* **32**, 107925 (2020).
9. Zhang, D. *et al.* 2-Deoxyglucose Reverses the Promoting Effect of Insulin on Colorectal Cancer Cells In Vitro. *PLoS One* **11**, e0151115 (2016).
10. Jeon, J. Y., Kim, S. W., Park, K. C. & Yun, M. The bifunctional autophagic flux by 2-deoxyglucose to control survival or growth of prostate cancer cells. *BMC Cancer* **15**, 623 (2015).
11. Ulmer, B. M. *et al.* Contractile Work Contributes to Maturation of Energy Metabolism in hiPSC-Derived Cardiomyocytes. *Stem Cell Reports* **10**, 834–847 (2018).
12. Correia, C. *et al.* Distinct carbon sources affect structural and functional maturation of cardiomyocytes derived from human pluripotent stem cells. *Sci. Rep.* **7**, 8590 (2017).
13. Hidalgo, A. *et al.* Modelling ischemia-reperfusion injury (IRI) in vitro using metabolically matured induced pluripotent stem cell-derived cardiomyocytes. *APL Bioeng.* **2**, 026102 (2018).
14. Kase, E. T. *et al.* Remodeling of Oxidative Energy Metabolism by Galactose Improves Glucose Handling and Metabolic Switching in Human Skeletal Muscle Cells. *PLoS One* **8**, e59972 (2013).
15. Yang, X. *et al.* Fatty Acids Enhance the Maturation of Cardiomyocytes Derived from Human Pluripotent Stem Cells. *Stem Cell Reports* **13**, 657–668 (2019).
16. Piquereau, J. *et al.* Postnatal development of mouse heart: Formation of energetic microdomains. *J. Physiol.* **588**, 2443–2454 (2010).
17. Piquereau, J. & Ventura-Clapier, R. Maturation of Cardiac Energy Metabolism During Perinatal Development. *Front. Physiol.* **9**, 1–10 (2018).
18. Zervou, S., J. Whittington, H., J. Russell, A. & A. Lygate, C. Augmentation of Creatine in the Heart. *Mini-Reviews Med. Chem.* **16**, 19–28 (2015).
19. Lopaschuk, G. D. & Jaswal, J. S. Energy Metabolic Phenotype of the Cardiomyocyte During Development, Differentiation, and Postnatal Maturation. *J. Cardiovasc. Pharmacol.* **56**, 130–140 (2010).
20. Ackers-Johnson, M. *et al.* A Simplified, Langendorff-Free Method for Concomitant Isolation of Viable

Cardiac Myocytes and Nonmyocytes From the Adult Mouse Heart. *Circ. Res.* **119**, 909–920 (2016).

21. Duan, Q. *et al.* Spermine ameliorates ischemia/reperfusion injury in cardiomyocytes via regulation of autophagy. *Am. J. Transl. Res.* **8**, 3976–3985 (2016).

22. Harris, S. P., Patel, J. R., Marton, L. J. & Moss, R. L. Polyamines decrease Ca 2+ sensitivity of tension and increase rates of activation in skinned cardiac myocytes. *Am. J. Physiol. Circ. Physiol.* **279**, H1383–H1391 (2000).

23. Lin, Y. *et al.* Polyamine Depletion Attenuates Isoproterenol-Induced Hypertrophy and Endoplasmic Reticulum Stress in Cardiomyocytes. *Cell. Physiol. Biochem.* **34**, 1455–1465 (2014).

24. Bakovic, M., Fullerton, M. D. & Michel, V. Metabolic and molecular aspects of ethanolamine phospholipid biosynthesis: the role of CTP:phosphoethanolamine cytidylyltransferase (Pcyt2). *Biochem. Cell Biol.* **85**, 283–300 (2007).

25. Bedada, F. B. *et al.* Acquisition of a Quantitative, Stoichiometrically Conserved Ratiometric Marker of Maturation Status in Stem Cell-Derived Cardiac Myocytes. *Stem Cell Reports* **3**, 594–605 (2014).

26. Poon, E. *et al.* Proteomic Analysis of Human Pluripotent Stem Cell-Derived, Fetal, and Adult Ventricular Cardiomyocytes Reveals Pathways Crucial for Cardiac Metabolism and Maturation. *Circ. Cardiovasc. Genet.* **8**, 427–436 (2015).

27. Parikh, S. S. *et al.* Thyroid and Glucocorticoid Hormones Promote Functional T-Tubule Development in Human-Induced Pluripotent Stem Cell-Derived Cardiomyocytes. *Circ. Res.* **121**, 1323–1330 (2017).

28. Yang, X. *et al.* Tri-iodo-l-thyronine promotes the maturation of human cardiomyocytes-derived from induced pluripotent stem cells. *J. Mol. Cell. Cardiol.* **72**, 296–304 (2014).

29. Kanda, M. *et al.* Leukemia Inhibitory Factor Enhances Endogenous Cardiomyocyte Regeneration after Myocardial Infarction. *PLoS One* **11**, e0156562 (2016).

30. Rupert, C. E. & Coulombe, K. L. K. IGF1 and NRG1 Enhance Proliferation, Metabolic Maturity, and the Force-Frequency Response in hESC-Derived Engineered Cardiac Tissues. *Stem Cells Int.* **2017**, 1–13 (2017).

31. Lu, C. *et al.* Demonstration of Direct Effects of Growth Hormone on Neonatal Cardiomyocytes. *J. Biol. Chem.* **276**, 22892–22900 (2001).

32. Xu, Y., Li, X., Liu, X. & Zhou, M. Neuregulin-1/ErbB Signaling and Chronic Heart Failure. *Adv. Pharmacol.* **59**, 31–51 (2010).

33. Noireaud, J. & Andriantsitohaina, R. Recent Insights in the Paracrine Modulation of Cardiomyocyte Contractility by Cardiac Endothelial Cells. *Biomed Res. Int.* **2014**, 923805 (2014).

34. Kobashigawa, L. C., Xu, Y. C., Padbury, J. F., Tseng, Y.-T. & Yano, N. Metformin Protects Cardiomyocyte from Doxorubicin Induced Cytotoxicity through an AMP-Activated Protein Kinase Dependent Signaling Pathway: An In Vitro Study. *PLoS One* **9**, e104888 (2014).

35. Kuppusamy, K. T. *et al.* Let-7 family of microRNA is required for maturation and adult-like metabolism in stem cell-derived cardiomyocytes. *Proc. Natl. Acad. Sci.* **112**, 201424042 (2015).

36. Zhao, Y. *et al.* A Platform for Generation of Chamber-Specific Cardiac Tissues and Disease Modeling. *Cell* **176**, 913-927.e18 (2019).

37. Churko, J. M. *et al.* Defining human cardiac transcription factor hierarchies using integrated single-cell heterogeneity analysis. *Nat. Commun.* **9**, (2018).

38. Giacomelli, E. *et al.* Human-iPSC-Derived Cardiac Stromal Cells Enhance Maturation in 3D Cardiac Microtissues and Reveal Non-cardiomyocyte Contributions to Heart Disease. *Cell Stem Cell* **26**, 862-879.e11 (2020).

39. Gilsbach, R. *et al.* Distinct epigenetic programs regulate cardiac myocyte development and disease in the

human heart in vivo. *Nat. Commun.* **9**, (2018).

40. Nakano, H. *et al.* Glucose inhibits cardiac muscle maturation through nucleotide biosynthesis. *Elife* **6**, e29330 (2017).

41. Gentillon, C. *et al.* Targeting HIF-1α in combination with PPARα activation and postnatal factors promotes the metabolic maturation of human induced pluripotent stem cell-derived cardiomyocytes. *J. Mol. Cell. Cardiol.* **132**, 120–135 (2019).